

# Species-specific features of ion channel localization in the parvalbumin interneuron in the human and mouse neocortex

Ph.D. dissertation

**Emőke Bakos**

Supervisors:

Dr. Karri Lamsa

Dr. Viktor Szegedi

Ph.D. School in Biology

Department of Physiology, Anatomy and Neuroscience

Faculty of Science and Informatics

University of Szeged



Hungarian Centre of Excellence for Molecular  
Medicine



Szeged

2026

## Introduction

The evolution of the neocortex was driven by genetic, epigenetic, and molecular changes that increased brain size, cortical folding, and microcircuit complexity. While core circuit motifs are conserved across mammals, their functional specialization diverged in response to ecological and behavioral demands. The layered organization of the neocortex enabled parallel processing, higher-order information integration, and greater cognitive flexibility. Comparisons between human and mouse cortical neurons reveal major differences in gene expression, ion channel composition, and interneuron diversity. Human GABAergic interneurons show greater variability, unique transcriptional signatures, and distinct electrophysiological properties, highlighting the limitations of rodent models for fully capturing human brain function. Parvalbumin-expressing (Pvalb) interneurons play a central inhibitory role by regulating excitatory-inhibitory balance, synchronization, and temporal precision. While their general features are conserved, human counterparts exhibit enhanced firing capacity and finer temporal control, supporting more complex cortical computations. In conclusion, the neocortex exemplifies the interplay of genetic, molecular, and structural innovations that enabled advanced cognitive abilities and human-specific neural adaptations.

Pvalb interneurons achieve their fast-spiking properties through a specialized set of ion channels that regulate excitability, firing precision, and synaptic integration. Key contributors include **HCN channels**, which stabilize membrane potential and enhance temporal fidelity; **Kir channels**, which set excitability thresholds and regulate resting potential; **Nav1.6 sodium channels**, concentrated at the axon initial segment to enable rapid action potential initiation and recovery; and **Kv1 potassium channels**, which ensure precise spike timing and prevent overexcitation. Comparative studies reveal species-specific differences in the expression, localization, and kinetics of these channels. For example, human neurons show stronger somatic HCN currents and lower AP thresholds due to Nav1.6 distribution, while rodents rely more on axonal HCN localization and Kir-mediated inhibition. These variations reflect evolutionary adaptations that tailor Pvalb interneurons to the computational demands of each species. In conclusion, the coordinated action of specialized ion channels underlies the unique fast-spiking excitability of Pvalb interneurons, with interspecies differences providing insights into both evolutionary neurobiology and the translational limitations of rodent models.

The axon initial segment (AIS) is a specialized neuronal domain where action potentials are initiated, defined by its dense ion channel clustering and unique cytoskeletal architecture. Its structural properties—such as length, location relative to the soma, and ion channel composition—determine neuronal excitability and firing precision. In parvalbumin (Pvalb) interneurons, the AIS supports low action potential thresholds and high temporal accuracy, enabling rapid inhibitory control. Species-specific differences in AIS morphology and Nav1.6 sodium channel density give human Pvalb interneurons lower thresholds and greater temporal precision compared to rodents, reflecting the higher computational demands of the human cortex. Kv1 potassium channels further shape spike timing, while  $\beta$ IV-spectrin and ankyrin-G scaffolding maintain AIS integrity and channel localization. In summary, the AIS represents an evolutionarily adaptable structure, tuned by channel distribution and cytoskeletal organization to support precise excitability and complex cortical computations across species.

## **Aims**

This doctoral research aimed to characterise the molecular, anatomical and electrophysiological properties of homologous interneuron types, specifically parvalbumin-expressing fast-spiking basket cells, in the human and mouse neocortex. By examining conserved neuron classes across species, the study aimed to identify adaptations unique to humans at the protein, genetic, and microcircuit levels. The specific research questions addressed include:

### **1. HCN Channel Localization and Function**

How does the subcellular distribution of hyperpolarization-activated cyclic nucleotide-gated (HCN) channels, particularly at the soma versus dendrites, differ between species? What are the electrophysiological consequences of this divergence?

### **2. Kir Channel Regulation of Excitability**

How does higher baseline input resistance in human Pvalb interneurons influence the functional effect of Kir (inward rectifier potassium) channel activation compared to mouse cells? Are there differences in the expression levels or membrane localization of Kir3.1 and Kir3.2 between species?

### **3. Axon Initial Segment (AIS) Specialization**

Can interspecies differences in AIS length, position, and ion channel composition account for variations in action potential thresholds and inhibitory control?

## Materials and Methods

This study employed multi-modal experimental and computational approaches to investigate the electrophysiological properties and ion channel distributions in cortical interneurons from both human and mouse tissue. All procedures were ethically approved by the University of Szeged Ethics Committee (ref. 75/2014) and conducted following Declaration of Helsinki guidelines, with written informed consent obtained from all patients or legal guardians prior to surgery.

**Tissue Preparation:** Human neocortical slices (350  $\mu\text{m}$ ) were obtained from frontal, temporal, or other cortical regions removed during surgical treatment of deep-brain targets in patients aged 20-82 years under standardized general anesthesia (midazolam, fentanyl, propofol, sevoflurane, rocuronium). Resected tissue was immediately immersed in ice-cold carbogen-aerated (95%  $\text{O}_2$ /5%  $\text{CO}_2$ ) slicing solution and rapidly transported to the laboratory in thermally insulated containers. Mouse transversal slices (350  $\mu\text{m}$ ) were prepared from somatosensory and frontal cortices of 5-7-week-old PVALBcre $\times$ Ai9 transgenic mice expressing tdTomato in parvalbumin-positive GABAergic neurons. All slices were incubated at room temperature (22-24°C) for 1 hour before gradual solution exchange to recording solution (higher  $\text{Ca}^{2+}$ : 3 mM, lower  $\text{Mg}^{2+}$ : 1.5 mM).

**Electrophysiology:** Whole-cell patch-clamp recordings were performed at 36-37°C using infrared DIC microscopy with micropipettes (5-8 M $\Omega$ ) filled with potassium gluconate-based solution containing biocytin (0.3% w/v). Recordings utilized a Multiclamp 700B amplifier with 6-8 kHz filtering and 35-50 kHz digitization, with appropriate compensations applied. Key parameters measured (from  $\geq 5$  repetitions each) included resting membrane potential, somatic leakage conductance (Ohm's law from -10 mV steps), input resistance (hyperpolarization to -90 mV), membrane time constant, and action potential threshold (10 mV/ms in phase plots). Pharmacological agents (ZD7288,  $\text{BaCl}_2$ , dendrotoxin-K) were applied via wash-in. Data were analyzed offline using pClamp 10.5, Spike2 8.1, OriginPro 9.5, and SigmaPlot 14.

**Computational Modeling:** A three-compartment biophysical model was constructed to assess HCN channel contributions to basket cell input-output responses. The model comprised a somatic compartment (400 M $\Omega$  resistance, 12 pF capacitance, -62 mV leak reversal) connected to cylindrical axonal and dendritic compartments (each 200  $\mu\text{m}$  length, 1.2  $\mu\text{m}$  diameter, 1.0 M $\Omega/\mu\text{m}$  longitudinal resistance, 12 fF/ $\mu\text{m}^2$  capacitance). Five voltage-dependent ionic currents were

incorporated: transient  $\text{Na}^+$ , delayed rectifying  $\text{K}^+$  (Kd), HCN, M-type  $\text{K}^+$ , and inward-rectifying  $\text{K}^+$  (Kir). Model parameters were iteratively optimized against experimental data to replicate characteristic response properties including rheobase and voltage sag amplitude.

**Histological Processing:** Following electrophysiological recording, biocytin-filled slices were fixed in 4% paraformaldehyde with 15% picric acid ( $\geq 12$  hours,  $4^\circ\text{C}$ ), embedded in 20% gelatin, sectioned to  $60\ \mu\text{m}$  using vibratome, and cryoprotected through sucrose treatment and freeze-thaw cycles. Neurons were visualized using fluorophore-conjugated streptavidin (Alexa 488 or Cy3, 1:1,000, 2.5 hours at  $22\text{--}24^\circ\text{C}$ ) for epifluorescence microscopy. Selected cells underwent DAB conversion using avidin-biotin-peroxidase complex with glucose oxidase-DAB-nickel visualization, followed by osmium treatment, uranyl acetate staining, ethanol dehydration, and Durcupan embedding for detailed three-dimensional reconstruction via Neurolucida system ( $100\times$  objective).

**Immunohistochemistry:** Free-floating sections underwent pepsin antigen retrieval (1 mg/mL in 1 M HCl,  $37^\circ\text{C}$ , 5-6 minutes), blocking with 20% horse serum, and sequential incubation with primary antibodies (1:100-1:1,000 dilutions) targeting parvalbumin, HCN1, HCN2, Kv3.1, spectrin beta-4, Nav1.6, Kv1.1, Kv1.2, GIRK1/Kir3.1, and GIRK2/Kir3.2 for three nights at  $4^\circ\text{C}$ , followed by appropriate fluorochrome-conjugated secondary antibodies overnight at  $4^\circ\text{C}$ .

**Microscopy:** Confocal imaging employed Nikon Eclipse Ti-E (with C2+ scan head) and Leica Stellaris 8 laser-scanning systems using high-NA objectives ( $\text{NA}=1.49$ ) with 488 nm, 561 nm, and 647 nm laser excitation. Super-resolution dSTORM was performed on a custom Nikon Ti-E platform with 647 nm excitation ( $2\text{--}4\ \text{kW}/\text{cm}^2$ ), 405 nm reactivation, and specialized GLOX oxygen-scavenging switching buffer containing 100 mM  $\beta$ -mercaptoethylamine, acquiring 20,000-25,000 frames per region with 20 ms exposure times and drift-corrected reconstruction via rainSTORM software (20 nm pixel size).

**Quantitative Fluorescence Analysis:** Multiple complementary approaches were employed depending on target protein localization. For somatic HCN and Kv3.1 channels: six radial measurement lines ( $8\ \mu\text{m}$  length,  $60^\circ$  angular spacing, 15 pixels/ $\mu\text{m}$ ) extended from soma center to extracellular space, with membrane zone defined as  $1\ \mu\text{m}$  width centered at half-maximum parvalbumin signal intensity, and measurements averaged across  $3\ \mu\text{m}$  intracellular,  $1\ \mu\text{m}$  membrane, and  $1\ \mu\text{m}$  extracellular regions. For Kir channels: 24 radial lines (50 pixels/ $\mu\text{m}$ ) were

aligned at membrane boundaries identified by parvalbumin signal onset, with intensity profiles normalized to maximum average and referenced to mean extracellular fluorescence (-3.0 to -0.5  $\mu\text{m}$  from membrane). For axon initial segment proteins: custom ImageJ macros measured beta-IV-spectrin-defined AIS length using Euclidean distance calculations, with Nav1.6, Kv1.1, and Kv1.2 fluorescence intensity profiles normalized into 10 bins along the AIS axis and referenced to somatic extracellular fluorescence values, maintaining consistent background subtraction across membrane (-0.5 to +0.5  $\mu\text{m}$ ), cytoplasmic (+0.5 to +1.5  $\mu\text{m}$ ), and axonal compartments.

**Patch-Sequencing:** Following electrophysiological characterization of fast-spiking neurons, nuclei were collected for transcriptomic analysis under RNase-free conditions (all surfaces treated with DNA AWAY™ and RNaseZap™). Nuclei were aspirated into the recording pipette using gentle negative pressure, expelled into PCR tubes containing lysis buffer (0.8% Triton X-100, 1 U/ $\mu\text{L}$  RNase inhibitor), and stored at -80°C. The RNase-free intracellular solution contained K-gluconate, ATP, GTP, phosphocreatine, EGTA, RNA-grade glycogen (20  $\mu\text{g}/\text{mL}$ ), and RNase inhibitor (0.5 U/ $\mu\text{L}$ ). cDNA libraries were prepared using SmartSeq2 protocol with 24 PCR amplification cycles, indexed, pooled equimolarly, and sequenced on Illumina MiSeq platform (50 base single-end reads, 1-2 million reads per sample). Sequencing reads (66-base paired-end) were aligned to GRCh38 (human) using STAR v2.7.11a with default parameters for SmartSeq analysis. Parvalbumin neuron identity was confirmed using the Allen Institute MapMyCells neuron type identification system: human cells were classified against the Seattle Alzheimer's Disease Brain Cell Atlas using Deep Generative Mapping, while mouse cells used the 10X Whole Mouse Brain reference with hierarchical mapping. Only cells classified as Pvalb neurons with bootstrapping probability >0.9 were included, with human samples showing subclass correlation coefficients >0.5 against the Allen Institute 10X Whole Human Brain dataset.

## Results

### Somatic HCN Channels speed up Spike Generation (Research study I)

This study reveals a fundamental species difference in the electrophysiological properties of fast-spiking GABAergic basket cells between human and mouse neocortex, centered on the differential expression and functional impact of hyperpolarization-activated cyclic nucleotide-gated (HCN) channels. Whole-cell current-clamp recordings from human fast-spiking interneurons

demonstrated a robust hyperpolarization-induced voltage sag during membrane potential steps from -70 mV to -90 mV, which was absent in the majority of mouse parvalbumin-positive (Pvalb) cells. Pharmacological blockade with ZD7288 (10  $\mu$ M) completely abolished this sag in human cells and induced a significant hyperpolarizing shift in resting membrane potential from a median of -62.0 mV to -68.75 mV ( $n = 22$ ), while producing no effect in mouse cells ( $n = 11$ ). This distinctive sag potential was remarkably consistent across human samples, showing no significant correlation with age (20-82 years), cortical region (frontal  $n=35$ , temporal  $n=24$ , other  $n=13$ ), sex, hemisphere, or underlying pathology, suggesting it represents a constitutive feature of human cortical fast-spiking interneurons.

Double immunofluorescence staining with parvalbumin and HCN1 or HCN2 antibodies, combined with quantitative confocal microscopy analysis of 2,340 radial intensity measurement lines from 390 cells, revealed striking species differences in HCN channel localization. Human Pvalb cells exhibited intense membrane enrichment of both HCN1 and HCN2 whereas mouse cells showed significantly weaker membrane signals with stronger intracellular localization suggesting cytoplasmic rather than membrane expression. Super-resolution dSTORM microscopy (spatial resolution  $<0.1 \mu\text{m}$ ) confirmed these findings, revealing concentrated HCN1 and HCN2 immunofluorescence in a narrow layer around human Pvalb cell soma with clear contrast between membrane and extra/intracellular compartments, while mouse cells displayed punctate cytoplasmic distribution rather than membrane localization.

Computational modeling using a multi-compartment neuron incorporating physiological HCN conductance (65% somatic, 35% dendritic based on outside-out recordings) demonstrated that somatic HCN channels produce a 5 mV depolarizing shift in resting potential, reduce the excitatory postsynaptic current (EPSC) amplitude threshold required for spike initiation, and progressively shorten EPSC-to-spike delay as HCN conductance increases from 0% to 150% of physiological levels. These simulations, validated against responses from representative cell h35 showing a 5-mV sag, reproduced the membrane dynamics, firing patterns, voltage dependence, and rebound firing observed experimentally under both baseline and ZD7288 conditions.

## **Kir Channels Regulate Subthreshold Excitability (Research study II)**

This study investigated the role of inward-rectifying potassium (Kir) channels in regulating subthreshold excitability of Pvalb fast-spiking interneurons in human and mouse neocortex,

revealing conserved functional mechanisms despite significant species differences in absolute membrane resistance. Whole-cell patch-clamp recordings applying square-pulse current steps (250-500 ms) from -70 mV demonstrated that human Pvalb neurons (n=34) possess significantly higher input resistance ( $R_{in}$ ) at all measured membrane potentials compared to mouse cells (n=25). Despite these absolute differences, both species displayed remarkably similar proportional decreases in  $R_{in}$  with membrane hyperpolarization, yielding comparable input rectification ratios (r $R_{in}$ ): human cells showed an 18.2% decrease in  $R_{in}$  at -90 mV compared to -60 mV, while mouse cells demonstrated a 23.8% decrease, with no statistical difference between species. Similar results were obtained using only hyperpolarizing steps from -60 mV, producing r $R_{in}$  values in humans (19.3% decrease) and in mice (22.6% decrease). All experiments were conducted in the presence of ZD7288 (10  $\mu$ M) to block HCN channels. Interestingly, r $R_{in}$  showed no correlation with initial  $R_{in}$  levels in human neurons (n=32), whereas mouse cells with higher  $R_{in}$  exhibited stronger rectification (n=25). Pharmacological blockade experiments confirmed that Kir channels mediate this input resistance rectification: extracellular application of barium ( $Ba^{2+}$ , 100  $\mu$ M) significantly reduced voltage-dependent  $R_{in}$  changes in both species by suppressing the  $R_{in}$  drop at hyperpolarized potentials. In human cells, r $R_{in}$  increased from baseline  $0.78 \pm 0.02$  to  $0.88 \pm 0.05$  after 10-minute  $Ba^{2+}$  wash-in (n=7, p=0.022), while in mouse cells r $R_{in}$  changed from  $0.81 \pm 0.02$  to  $0.90 \pm 0.06$  (n=9, p=0.009), with no species difference in  $Ba^{2+}$  effect.

Molecular characterization using patch-sequencing revealed that among 15 KCNJ genes encoding Kir channels, KCNJ3 and KCNJ6 (encoding Kir3.1 and Kir3.2 respectively) showed the most robust mRNA expression in both human (n=21) and mouse (n=10) Pvalb neurons. Species-specific expression patterns emerged for KCNJ4 (encoding Kir2.3, abundant in human but absent in mouse) and KCNJ9 (encoding Kir3.3, abundant in mouse but low in human). Analysis of transcriptomic data from the Allen Brain Institute's human middle temporal gyrus database confirmed elevated Kir3.1 and Kir3.2 mRNA levels in both species, while KCNJ9 was robustly expressed in mouse but absent in human, and KCNJ4 showed the opposite pattern.

Double immunofluorescence staining combined with confocal and dSTORM super-resolution microscopy definitively localized Kir3.1 and Kir3.2 proteins to the somatic membrane of both human and mouse Pvalb neurons. Quantitative analysis using radial immunofluorescence intensity profiles (24 lines per sample, spanning 5  $\mu$ m from soma center to 3  $\mu$ m extracellular)



demonstrated peak fluorescence intensity for both Kir3.1 and Kir3.2 at the plasma membrane zone where Pvalb (or tdTomato in transgenic mice) signal rapidly decreased. dSTORM imaging revealed individual fluorophore signals localized to the extracellular membrane surface, confirming membrane expression of both channel subtypes.

Computational modeling using a multi-compartment Pvalb neuron incorporating passive leak conductance, HCN current, Kv7- and Kv1-type potassium currents, and Hodgkin-Huxley action potential mechanisms successfully replicated the electrical properties observed in actual neurons (model neuron H4). Simulations varying passive leak conductance (1-11 nS) and Kir conductance (0-20 nS, with ~10% active at -70 mV and ~90% at -90 mV) demonstrated that neurons with lower passive leak conductance require less Kir conductance to achieve the same  $rR_{in}$  observed in cells with higher leak conductance, explaining the conserved rectification ratio across the wide range of absolute  $R_{in}$  values measured in human and mouse Pvalb neurons.

### **AIS Geometry and Kv1 Channels Shape AP Threshold (Research study III)**

This comprehensive study investigated the structural and molecular mechanisms underlying species differences in action potential (AP) firing threshold between human and mouse Pvalb fast-spiking interneurons, revealing that human neurons compensate for slower membrane kinetics through elongated axon initial segments (AIS) and reduced inhibitory Kv1 potassium channel expression. Whole-cell current-clamp recordings from 80 human Pvalb neurons (from 62 patients aged 11-85 years, sampled from frontal  $n=36$ , temporal  $n=20$ , and other cortical regions  $n=24$ ) and 80 mouse neurons demonstrated that human cells exhibit significantly lower AP firing thresholds compared to mouse cells, with no variation across cortical regions (frontal vs. temporal, sex, or age). Electrophysiological characterization revealed that human Pvalb neurons possess significantly higher somatic input resistance ( $n=50$ ) compared to mouse neurons ( $n=40$ ), while membrane capacitance showed no species difference, resulting in slower membrane time constants ( $\tau$ ) in human cells versus mouse cells. Critically, both species exhibited a strong negative correlation between slow membrane  $\tau$  and low AP firing threshold when data were pooled ( $n=90$ ), demonstrating that neurons with slower  $\tau$  achieve lower AP thresholds as a compensatory mechanism.

Anatomical characterization using beta-IV-spectrin immunohistochemistry and three-dimensional confocal microscopy revealed significant species differences in AIS morphology: while the distance from AIS initiation to soma was similar between species, human Pvalb neurons possessed significantly longer AIS versus mouse, resulting in more distal AIS termination sites in humans. Analysis of 13 human and 14 mouse biocytin-filled, electrophysiologically characterized neurons with complete AIS recovery confirmed longer AIS in human cells and more distal termination. Importantly, when pooling data from both species, significant correlations emerged between AP threshold and AIS position: distance from initiation site to soma and distance from termination site to soma, while AIS length alone showed no correlation, indicating that distal AIS positioning rather than absolute length primarily determines threshold differences. Axon diameter measurements at five locations (two pre-AIS, three within AIS) in biocytin-filled neurons revealed no species differences and no correlation with AP threshold in either segment, excluding axon caliber as a contributor to threshold differences.

Analysis of voltage-gated sodium channel Nav1.6 distribution using triple immunofluorescence and quantitative confocal microscopy showed robust, uniform immunoreactivity throughout the AIS in both species (human F-Fex.c. 73.18, n=21; mouse 48.40, n=26) with no preferential localization to distal AIS regions and similar weak expression in pre-AIS and post-AIS segments, demonstrating that Nav1.6 distribution patterns do not explain species differences. Triple immunofluorescence analysis of Kv1.1 potassium channels revealed striking species divergence: mouse Pvalb neurons showed robust Kv1.1 immunoreactivity in the AIS (F-Fex.c. 47.56, n=31), whereas human cells exhibited weak or absent AIS expression despite strong labeling in neighboring Pvalb-negative neurons, with uniform distribution when present. Somatic membrane analysis confirmed Kv1.1 absence in human cells (F-Fex.c. -1.23, n=31) versus presence in mouse cells (5.42, n=31). Kv1.2 channel analysis showed no species difference in AIS expression (human 2.95, n=60 vs. mouse 17.04, n=30) but slightly higher somatic membrane expression in humans.

Patch-sequencing analysis of 21 human and 16 mouse Pvalb neurons (identified by Allen Institute neuron type classification) revealed complete absence of KCNA1 mRNA (encoding Kv1.1) in all 21 human cells versus robust expression in 7 of 16 mouse cells, while KCNA2 mRNA

(encoding Kv1.2) showed similar expression levels. Analysis of Allen Brain Institute transcriptomic databases confirmed these findings.

Pharmacological experiments using dendrotoxin-K (DTXK, 100 nM, 10-minute wash-in), a specific Kv1 channel blocker, revealed differential effects: in mouse neurons, DTXK induced substantial threshold hyperpolarization ( $n=15$ ) and decreased rheobase current, while human neurons showed minimal threshold shift ( $n=11$ ) with no rheobase change, confirming significantly different species responses. DTXK also reduced AP afterhyperpolarization amplitude and increased input resistance in mice but not humans, eliminated baseline species differences in AP half-width and membrane tau, and equally reduced AP peak amplitude in both species.

Computational modeling of a Pvalb neuron incorporating voltage-sensitive axonal Nav1.6, high-threshold somatic Nav1.2, Kv3.1/3.2, voltage-independent leak, M-type, Kir-type, and Ih currents demonstrated that varying AIS length (10-30  $\mu\text{m}$ ) with fixed Nav1.6 and Kv1 densities (20 nS/ $\mu\text{m}^2$  each) progressively lowered AP threshold, while increasing Kv1 density (0-15 nS/ $\mu\text{m}^2$ ) at fixed 20  $\mu\text{m}$  AIS length elevated threshold. Synaptic stimulation simulations with excitatory postsynaptic currents (6-11 nS conductance) at -70 mV revealed that human-type AIS (30  $\mu\text{m}$  length, 0 nS/ $\mu\text{m}^2$  Kv1) versus mouse-type AIS (10  $\mu\text{m}$  length, 20 nS/ $\mu\text{m}^2$  Kv1) reduced EPSP-to-AP latency despite slower membrane tau, with minimum and maximum latencies of 4.8 ms and 7.8 ms respectively at fixed 8.5 nS EPSC strength.

## Discussion

### Research study I: Somatic HCN channels facilitate the input-output transformation in human fast-spiking interneurons

This study reveals that human neocortical fast-spiking basket cells possess somatic **HCN (hyperpolarization-activated cyclic nucleotide-gated)** channels, which are largely absent in rodents. These channels create a distinctive **voltage sag** during hyperpolarization, confirmed through electrophysiological and immunohistochemical methods showing **HCN1 and HCN2** localization in human **parvalbumin-expressing (Pvalb)** interneuron soma. Functionally, these somatic HCN channels **compensate for the slower passive membrane properties** of human neurons, enabling rapid conversion of synaptic inputs into action potentials—essential for effective inhibitory signaling. Computational models show that HCN conductance **enhances EPSP-to-spike**

**coupling speed** and increases neuronal responsiveness. Moreover, HCN channels in human neurons are subject to **neuromodulatory control**, allowing dynamic adjustment of excitability through intracellular signaling. This flexibility likely helps neurons adapt to varying network demands.

Comparative findings in **macaque interneurons** suggest that somatic HCN expression is a **primate-specific adaptation**, supporting efficient cortical processing despite increased circuit complexity. Ultimately, these channels improve **temporal precision and synchronization** in cortical networks, representing an **evolutionary advantage** in primate brain function.

### **Research study II: Kir channels similarly regulate intrinsic excitability in human and mouse Pvalb neurons despite their different input resistances**

This study examined how **inward-rectifier potassium (Kir) channels** regulate the excitability of **Pvalb interneurons** in humans and mice. Despite the **higher input resistance** of human neurons, both species showed **similar voltage-dependent decreases** in resistance during hyperpolarization—a hallmark of Kir channel activity, which was abolished by **barium**. **Gene expression and imaging analyses** confirmed strong **Kir3.1 and Kir3.2** expression and **somatic membrane localization** in both species. While humans displayed higher overall expression, mouse neurons expressed a more **diverse set of Kir subunits**. **Computational modeling** revealed that human neurons need **less Kir conductance** to achieve the same rectifying effect as mouse neurons, reflecting an **energy-efficient mechanism** suited to their higher passive membrane resistance. This efficiency may help fast-spiking interneurons conserve **metabolic energy** while maintaining rapid inhibitory control. Functionally, Kir channels contribute to both **hyperpolarization** and **shunting inhibition**, which reduce neuronal excitability and dampen excitatory inputs. Their activity is **modulated by opioid and GABA-B receptors**, providing a flexible mechanism for neuromodulatory control.

Finally, the study observed **cell-to-cell variability** in Kir-mediated inhibition, particularly in human neurons, suggesting possible differences in **channel expression or plasticity**. Overall, Kir channels represent a **conserved inhibitory mechanism** across species, with **human-specific adaptations** that enhance efficiency and regulatory flexibility within complex cortical networks.

### **Research study III: AIS adaptations set a lower AP threshold in human Pvalb neurons**

This study found that **human Pvalb interneurons** exhibit a **lower action potential (AP) threshold** compared to rodent neurons. This adaptation is crucial, as human interneurons have **slower membrane time constants** and **higher input resistance**, which would normally hinder rapid firing. The lower AP threshold therefore acts as a **compensatory mechanism** that preserves fast and reliable spiking despite these passive electrical constraints. Two major factors underlie this enhanced excitability: an **elongated axon initial segment (AIS)** and **reduced expression of Kv1-type potassium channels**. Immunohistochemistry revealed that the human AIS is **significantly longer** than in mice, providing more surface area for **voltage-gated sodium channel clustering** and facilitating AP initiation. At the same time, human neurons show **minimal expression of Kv1.1 and Kv1.2 channels**, which normally act to **raise the firing threshold**. Computational modeling confirmed that this combination—**longer AIS + reduced Kv1 conductance**—substantially **lowers the AP threshold** in human neurons. Notably, the **position** of the AIS relative to the soma and the **axon diameter** were similar between species, indicating that the enhanced excitability arises from **molecular and structural specialization**, not geometric differences. The study also suggests that **AIS plasticity**, involving changes in its length or ion channel composition, could contribute to **cell-to-cell variability** in firing thresholds among human interneurons.

Overall, these findings indicate that **human Pvalb neurons have evolved specific AIS adaptations** that maintain **fast-spiking performance** and **temporal precision** despite slower membrane properties. By lowering the AP threshold through AIS elongation and reduced potassium channel expression, human interneurons sustain the **speed and reliability** required for efficient cortical inhibition in complex neural circuits. These findings establish that human Pvalb interneurons achieve faster input-output performance than their slower membrane kinetics would predict through evolutionary adaptations in AIS geometry (elongation and distal positioning) and molecular composition (virtual elimination of threshold-elevating Kv1.1 channels), providing a mechanism for maintaining rapid cortical inhibition while accommodating the biophysical constraints of larger, higher-resistance neurons.

## Összefoglalás

Az emberi és egér agykérgi gyorsan tüzelő gátló idegsejtek (kosársejtek) összehasonlító vizsgálata jelentős faji különbségeket tárt fel. Az emberi kosársejtek szómájában nagymértékben expresszálódnak a HCN1 és HCN2 ioncsatornák, amelyek rágcsőcsatlakozásokban hiányoznak. Ezek a csatornák felgyorsítják a membránpotenciál változásait és csökkentik a gerjesztő jelzések és az akciós potenciál kialakulása közötti időt, kompenzálva az emberi neuronok lassabb alapvető membrándinamikáját.

Az emberi interneuronok nagyobb bemeneti ellenállással rendelkeznek az alacsonyabb ionáteresztés miatt, így erősebben reagálnak szinaptikus jelzésekre. A Kir3.1 és Kir3.2 káliumcsatornák mindkét fajban szabályozzák a küszöbérték alatti gerjeszthetőséget, azonban az emberi sejtekben hatékonyabb működést tesznek lehetővé.

További különbség, hogy az emberi gyorsan tüzelő neuronok hosszabb axon kezdeti szegmenssel (AIS) rendelkeznek, és hiányoznak belőlük a Kv1.1 és Kv1.2 káliumcsatornák, amelyek egerekben jelen vannak. Ez az eltérő szerkezet alacsonyabb akciós potenciál küszöböt eredményez.

Összességében az emberi neokortikális gátló interneuronok specifikus szerkezeti és molekuláris adaptációi – a szomatikus HCN-csatornák, a kiterjesztett AIS és az eltérő ioncsatorna-expresszió – lehetővé teszik a gyors, pontos gátló jelátvitelt a nagyobb és összetettebb emberi agykéregben, kompenzálva a lassabb passzív membrántulajdonságokat.

## List of Publications

MTMT ID: 10088219

Cumulative IF: **18.9** (24)

### Publications Related to Thesis

**HCN channels at the cell soma ensure the rapid electrical reactivity of fast-spiking interneurons in human neocortex**

Viktor Szegedi\*, **Emőke Bakos\***, Szabina Furdan, Bálint H. Kovács, Dániel Varga, Miklós Erdélyi, Pál Barzó, Attila Szücs, Gábor Tamás, Karri Lamsa

PLOS BIOLOGY (1544-9173 1545-7885): 21 (2) Paper e3002001. 33 p. (2023)  
doi:10.1371/journal.pbio.3002001. **IF: 7.8**

**Adaptations of the axon initial segment in fast-spiking interneurons of the human neocortex support low action potential thresholds**

**Emőke Bakos\***, Ádám Tiszlavicz\*, Viktor Szegedi, Abdenmour Douida, Szabina Furdan, Daphne K. Welter, Jonathan M. Landry, Balázs Bende, Gábor Hutóczki, Pál Barzó, Gábor Tamás, Vladimir Benes, Attila Szücs, Karri Lamsa

PLOS BIOLOGY (1544-9173 1545-7885): 23 (12) Paper e3003549. 35 p. (2025)  
doi:10.1371/journal.pbio.3003549. **IF: 7.2**

**Regulation of input excitability in human and mouse parvalbumin interneurons by Kir potassium channels**

Szabina Furdan\*, Abdenmour Douida\*, **Emőke Bakos**, Ádám Tiszlavicz, Gábor Molnár, Gábor Tamás, Daphne Welter, Jonathan Landry, Bálint H. Kovács, Miklós Erdélyi, Balázs Bende, Gábor Hutóczki, Pál Barzó, Vladimir Benes, Viktor Szegedi, Attila Szücs, Karri Lamsa

BioRxiv [Preprint]. 16:2025.04.11.648314. (2025) doi:10.1101/2025.04.11.648314.

Submitted to Communications Biology (IF: 5.1)

### **Other Publication**

#### **Aging-associated weakening of the action potential in fast-spiking interneurons in the human neocortex**

Viktor Szegedi\*, Ádám Tiszlavicz, Szabina Furdan, Abdenmour Douida, **Emőke Bakos**, Pál Barzó, Gábor Tamás, Attila Szűcs, Karri Lamsa

JOURNAL OF BIOTECHNOLOGY (0168-1656 1873-4863): 389 pp 1-12 (2024)  
doi:10.1016/j.jbiotec.2024.04.020. **IF: 3.9**

### **Conferences**

#### **HCN channels at the somatic membrane ensure rapid input–output function of human neocortex fast-spiking interneurons**

Viktor Szegedi, Emőke Bakos, Szabina Furdan, Bálint Kovács, Dániel Varga, Miklós Erdélyi, Pál Barzó, Attila Szűcs, Gábor Tamás, Karri Lamsa

Joint Meeting of the Hungarian Neuroscience Society (MITT) and the Austrian Neuroscience Association (ANA), Budapest, Hungary 2023. Poster presentation.

#### **HCN-channels at soma membrane are pivotal to rapid input-output function of human neocortical fast-spiking interneurons**

Viktor Szegedi, Emőke Bakos, Szabina Furdan, Bálint Kovács, Dániel Varga, Miklós Erdélyi, Pál Barzó, Attila Szűcs, Gábor Tamás, Karri Lamsa

Federation of European Neuroscience Societies (FENS) Regional Meeting, Algarve, Portugal 2023. Poster presentation.

#### **Low firing threshold shortens action potential generation delay in human fast-spiking interneurons**

Emőke Bakos, Ádám Tiszlavicz, Viktor Szegedi, Abdenmour Douida, Pál Barzó, Gábor Tamás, Attila Szűcs, Karri Lamsa

International Neuroscience Conference (INC), Pécs, Hungary 2024. Poster presentation.



**Low action potential firing threshold facilitates “in–out” -function of fast-spiking interneurons in the human neocortex**

Emőke Bakos, Ádám Tizslavicz, Viktor Szegedi, Abdenmour Douida, Daphne Welter, Jonathan Landry, Pál Barzó, Gábor Tamás, Vladimir Benes, Attila Szücs, Karri Lamsa

Federation of European Neuroscience Societies (FENS) Forum, Vienna, Austria 2024.  
Poster presentation.

**Ion channel localisation differences explain distinct electrical excitability of fast-spiking neurons in the human and rodent neocortex**

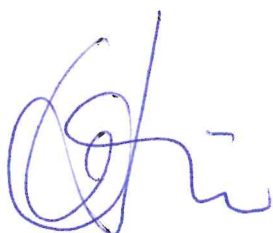
Emőke Bakos, Ádám Tizslavicz, Viktor Szegedi, Abdenmour Douida, Szabina Horváth-Furdan, Daphne Welter, Jonathan Landry, Pál Barzó, Gábor Tamás, Vladimir Benes, Attila Szücs, Karri Lamsa

Federation of European Neuroscience Societies (FENS) Regional Meeting, Oslo, Norway 2025. Poster presentation.

## Declaration

We, the undersigned Dr. Karri Lamsa and Dr. Viktor Szegedi, as the subject supervisors of the candidate, hereby certify that Emőke Bakos Ph.D. candidate has made a significant contribution to the preparation of the above-mentioned scientific publications. The results of her thesis will not be used in any other doctoral thesis. We declare that the results of the experiments carried out by the candidate have not been used by ourselves and the other co-authors to obtain the degree and will not be used in the future.

Szeged, February 10, 2026



Dr. Karri Lamsa



Dr. Viktor Szegedi